An Efficient Fan Drive System Based on a Novel Hydraulic Transmission

Feng Wang and Kim A. Stelson

***Abstract*—An efficient fan drive system based on a novel pressure-controlled hydraulic transmission (PCT) is studied in this paper. The new transmission uses a double-acting vane pump with a floating ring. By coupling the floating ring to an output shaft, the vane pump becomes a hydraulic transmission. The new transmission combines pumping and motoring functions in one unit, making it much simpler than conventional hydrostatic transmission (HST). By controlling the pressure in the PCT, the output shaft torque and speed can be adjusted. In this paper, the fundamental principle of the new transmission is studied, with the focus on how the output shaft torque is influenced by the control pressure. To demonstrate its advantage, the new transmission is applied to a fan drive system, and the transmission efficiency is compared to a HST. Experimental results show that the input power of the fan drive system with the PCT is lower than that with an HST. By feeding the control flow to a hydraulic motor coupled to the output shaft of the PCT, a pressure-controlled hydromechanical transmission is constituted and the test result shows higher transmission efficiency than a PCT.**

***Index Terms*—Construction machinery, cooling fan system, hydrostatic fan drive, hydrostatic transmission (HST), pressure-controlled hydraulic transmission (PCT).**

I. Introduction

It is desired to reduce the fuel consumed by off-road equipment for construction, agriculture, and forestry. Most of these machines are powered by diesel engines due to high power and torque demands. Mobile equipment manufacturers are required to meet Tier 4 engine emissions regulations, calling for 50–90% reduction in particulate matter emission and up to 90% reduction in emissions of oxides of nitrogen [1].

Mobile equipment manufacturers are going through a series of innovations as the emission regulations demand cleaner and cleaner exhaust. Some technologies such as exhaust gas recirculation and selective catalytic reduction help to meet these requirements but increase engine cooling requirements [2]. Under normal conditions, approximately 30% of the engine power is converted to mechanical power with the rest becoming heat. Of the energy converted to heat, 35% to 45% is lost directly to the atmosphere. The remaining must be rejected by a cooling fan system [3], [4]. Improving fan drive efficiency makes a significant contribution to machine efficiency [5]–[7]. An efficient engine requires both precise temperature control and a more efficient fan drive.

Manuscript received May 16, 2014; revised August 8, 2014; accepted October 27, 2014. Recommended by Technical Editor Prof. Y. Li. This work was supported by the Center for Compact and Efficient Fluid Power, a National Science Foundation Engineering Research Center supported by a cooperative agreement no. EEC-0540834, at the University of Minnesota.

The authors are with the Center for Compact and Efficient Fluid Power, Department of Mechanical Engineering, University of Minnesota, Minneapolis, MN 55455 USA (e-mail: wang2148@umn.edu; kstelson@umn.edu).

Color versions of one or more of the figures in this paper are available online at http://ieeexplore.ieee.org.

Digital Object Identifier 10.1109/TMECH.2014.2370893

There are different types of fan drives in the market today: mechanical, electrical, and hydraulic fan drives. Direct engine drive, pulley and belt drive, and clutch drive are types of mechanical drives. Electrical drives use an electric motor to drive the fan. Hydraulic fan drives, including viscous and hydrostatic drives, use fluid to transfer power or torque. The former uses viscous drag of the fluid to transfer the torque, while the latter uses fluid pressure.

Fan drives have traditionally been mechanical, using pulleys and a belt between the engine and the fan. The drive ratio is selected to provide adequate cooling within the engine speed range. Because of its simple but crude control, mechanical fan systems usually overcool to ensure adequate cooling at maximum heat rejection. In mechanical fan systems, the fan speed does not respond to engine coolant temperature directly, severely limiting the cooling accuracy and efficiency [8]. Theoretically, fan power is proportional to the cube of the fan speed. By reducing the fan speed by 10%, the fan power can be reduced by 27% [9].

A more efficient way to control the fan is to adjust the fan speed proportional to the cooling requirement and, independently, of the engine speed. This provides adequate cooling at all conditions, while minimizing fan speed to avoid excessive fan power consumption [10]–[12]. Electric and hydraulic drives have variable fan speed. Electric and viscous drives are mainly used for low- or medium-power applications. For heavy duty off-road vehicles, a temperature-activated electronically-controlled hydrostatic fan drive offers a practical solution, where the fan speed can be precisely modulated to cooling requirements under widely varying operating conditions [13].

There are also some other advantages of the hydrostatic fan drive. Smooth modulation avoids large fan speed acceleration, sudden changes in noise, and excessive shock loading to the system. If properly sized, the fan normally operates at medium speed, giving a low-noise level. By properly routing the hydraulic lines, the hydrostatic fan drive can be located in any desired position. The ability to reverse the fan rotation is especially beneficial for agricultural applications, since it can clean the cooling fan and improve the cooling efficiency.

Hydrostatic fan drives occur in different forms. A simple and cost-effective form is to use a fixed displacement pump to drive a fixed displacement motor and use a pressure relief valve across the motor to control the fan speed. According to the fan power law, the fan shaft torque is proportional to the square of the fan speed. The fan speed is determined by the motor differential pressure set by the pressure relief valve. The pump is sized to meet the flow demand at the maximum fan speed. For lower fan speeds, the excess flow is bypassed through relief valve, resulting in severe losses [14]. A more efficient solution is to use a pressure-compensated variable displacement pump to drive a fixed displacement motor. The pump only needs to provide the amount of flow needed by the fan and there is no bypass relief valve in the system [15], [16]. This is efficient since the pump automatically adapts to the flow requirement by adjusting its displacement.

Although the hydrostatic fan drive has been proven to be an efficient solution for heavy duty machines, the hydrostatic drive itself is still inefficient due to the pump and motor inefficiencies. The pump efficiency drops considerably at partial displacement, a normal condition when the fan runs at moderate speed. Line losses and additional charge power for a closed circuit further lowers the overall efficiency of the hydrostatic drive. Moreover, the initial cost of this drive is relatively high due to the costly variable displacement pump.

In this paper, a more efficient and cost-effective fan drive based on a novel hydraulic transmission is introduced. The new transmission uses a double-acting vane pump with a floating ring. By coupling the floating ring to an output shaft, the vane pump becomes a hydraulic transmission [17]. The new transmission combines the pumping and motoring functions in one unit, eliminating the parasitic and line losses, and making the whole unit more compact and efficient. Unlike a conventional hydrostatic transmission (HST), where the transmission ratio is adjusted by changing the displacement of either the pump, motor, or both, the ratio of this new transmission is adjusted by controlling the pressure, making it a pressure-controlled hydraulic transmission (PCT). In this paper, the principle and the steady-state characteristics of the PCT are studied. The transmission efficiency of the PCT is compared with a conventional HST in a fan drive system.

II. Pressure-Controlled Hydraulic Transmission

A. Overview

The schematic of the PCT and its hydraulic symbol are shown in Fig. 1. The hydraulic symbol is newly proposed to reflect the fact that it has a floating ring. The design is based on a double-acting vane pump since it has a balanced design and, therefore, a longer lifetime and quieter operation than a gear or piston pump [18]. The rotor with the vanes is coupled to the input shaft, and the floating ring is coupled to the output shaft. As it is based on a double-acting vane pump, the PCT intakes and discharges oil twice in one shaft revolution.

The new transmission combines both the pumping and motoring function in one single unit, making it function like a conventional HST. The pumping unit, consisting of the input shaft, rotor/vane assembly, and the floating ring, is the same as a conventional vane pump except for the floating ring. The motoring unit consists of the floating ring and the output shaft coupled to it. The fluid pressure inside the PCT acts on the pumping and motoring unit simultaneously, thus transfers the power. Compared to a conventional HST, the PCT reduces the parasitic losses in the pump and motor and eliminates the line losses in between, making the unit simpler and more efficient.

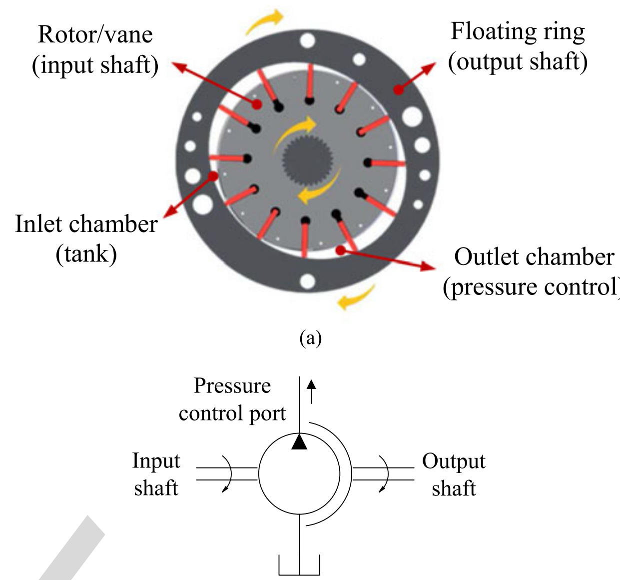

Fig. 1. Schematic of PCT and its hydraulic symbol. (a) Structure. (b) Hydraulic symbol.

Unlike a conventional HST where the transmission ratio can be adjusted by changing the displacement of the pump, the motor, or both, the ratio of the PCT is adjusted by changing the pressure at the control port. By changing the control pressure, the output shaft torque and speed can be adjusted. The pressure control in this new transmission achieves the same function as the displacement control in a conventional HST but with a simpler structure.

B. Flow Characteristic

The control flow at the control port Q_c is determined by the relative rotary speed between the input and output shaft

$$Q_c = (\omega_p - \omega_m) D_{pm} \eta_v \tag{1}$$

where ω_p and ω_m are the input and output shaft speeds, D_{pm} is the displacement of the PCT, $\eta_v = f(p_c, \omega_p - \omega_m)$ is the volumetric efficiency of the transmission, which is pressure and relative speed dependent, and p_c is the control pressure at the control port. The control pressure is normally regulated by a pilot or remotely controlled relief valve.

With a relief valve set at the control port, the PCT always discharges oil to the control port and never absorbs oil from the control port since the relief valve is a power consumer instead of a power source. This indicates that the control flow shown in Fig. 1 is always positive. This comes to the conclusion that with a passive pressure control such as relief valve pressure control, the output shaft never turns faster than the input shaft $(\omega_p \geq \omega_m)$ according to (1).

In an extreme condition when the control port is plugged and the control flow is zero, the input and output shafts have the same rotary speeds according to (1). This turns the PCT to a

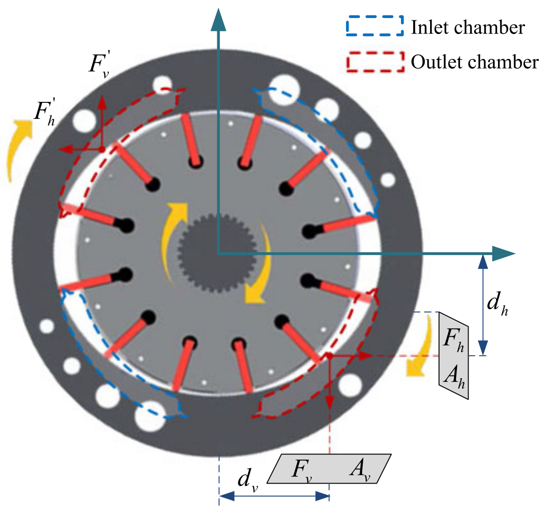

Fig. 2. Hydraulic torque acting on the floating ring in the PCT.

direct drive, where the trapped fluid between the rotor and the ring is pressurized, efficiently transferring the torque between the input and output shafts. This is an attractive feature of the PCT, a feature that is absent from an HST.

Similar to an induction motor, a slip is defined between the input and output rotary speed

$$s_{pm} = \frac{\omega_p - \omega_m}{\omega_p}. \tag{2}$$

C. Output Shaft Torque Analysis

The PCT controls the output shaft torque by controlling the pressure at the control port. There are two driving torques on the PCT output shaft: hydraulic torque and viscous torque.

1) Hydraulic Torque: In a double-acting vane pump, the rotor contour and the ring outer contour are concentric. The ring inner contour is not circular and consists of several arcs. As the rotor turns, the vanes are forced to turn and the vane tips follow the ring inner contour either by centrifugal force, spring force, or pressure force on the vane bottom. The ring inner contour is designed so that the pump intakes and discharges oil twice per rotor revolution. There are two inlet chambers and two outlet chambers in a double-acting vane pump. These chambers are symmetric. The fluid pressure in the outlet chambers acts on the floating ring and generates the hydraulic torque. The schematic of the hydraulic torque acting on the floating ring is illustrated in Fig. 2.

In this analysis, it is assumed that the rotor turns clockwise. In Fig. 2, the two blue kidneys show inlet chamber areas, and the two red kidneys show outlet chamber areas. The inlet chambers are vented to tank with zero pressure, and the outlet chambers are vented to the control port shown in Fig. 1. The fluid pressure in the outlet chambers rotates the floating ring. Taking the outlet chamber in the fourth quadrant for instance, the hydraulic force acting on the ring is decomposed into horizontal and vertical components F_h and F_v

$$F_h = p_c A_h \tag{3}$$

$$F_v = p_c A_v \tag{4}$$

where A_h and A_v are the horizontal and vertical projected areas.

The horizontal and vertical components of the hydraulic force act on the center of their projected areas as the pressure is evenly distributed on the projected area. The horizontal hydraulic force generates anticlockwise torque, while the vertical hydraulic force generates clockwise torque.

Since the two inlet chambers and two outlet chambers are symmetric, the same force analysis applies to the second quadrant ($F_h = F_h', F_v = F_v'$). Therefore, the hydraulic torque generated by these hydraulic forces T_h is

$$T_h = 2\left(F_v d_v - F_h d_h\right) = 2p_c\left(A_v d_v - A_h d_h\right) \tag{5}$$

where d_h and d_v are the moment arms of the horizontal and vertical forces.

Since the PCT design is based on a conventional double-acting vane pump except that it has a rotating ring, the hydraulic torque analysis on the rotating ring is essentially the same as that in a vane pump. The ring inner contour consists of several curves with the long axis greater than the minor axis. The clockwise and counterclockwise torques cannot be cancelled and, thus, the hydraulic torque is generated.

The projected areas (A_h and A_v) and force moment arms (d_h and d_v) are not only determined by the ring inner contour, but also determined by the size and position of the inlet chamber kidney slot and, therefore, is case dependent. Different vane pump manufacturers may have different pump designs. Instead of giving a case study, the hydraulic torque analysis in this section intends to give a general description on how the hydraulic torque is generated in the PCT. Based on the design of the double-acting vane pump, it yields to $A_v d_v > A_h d_h$. This means the generated hydraulic torque has the same direction as the rotor speed.

According to (5), the hydraulic torque generated by the fluid pressure is proportional to the control pressure. The fluid pressure also acts on the rotor/vane assembly, generating a reaction torque on the input shaft. The hydraulic torque on the floating ring and the reaction torque on the input shaft are equal since they are action–reaction pairs.

Based on (5), the geometry displacement of the PCT is

$$D_{pm} = \frac{T_h}{p_c} = 2\left(A_v d_v - A_h d_h\right). \tag{6}$$

This displacement is the theoretical displacement of the PCT and is geometry dependent.

2) Viscous Torque: Another torque that drives the floating ring is the viscous torque as illustrated in Fig. 3. There is an oil film along the ring inner surface as shown with the orange curve in Fig. 3(a). The two boundary layers of the oil film are driven by the ring inner surface and the vane tips, respectively. Due to the rotary speed difference between the rotor and the floating ring, there is relative speed between two layers. This is similar to the oil film between two parallel surfaces with relative motion.

Fig. 3(b) shows the oil film, where the upper layer has a speed of U and the bottom layer is stationary. The oil film has zero

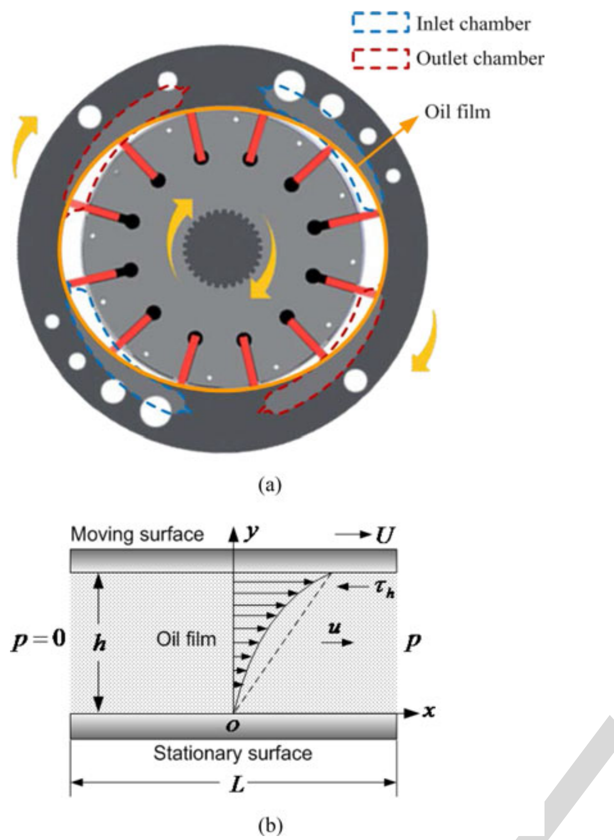

Fig. 3. Viscous torque acting on the floating ring in the PCT. (a) Oil film on the ring inner contour. (b) Oil-film velocity profile between two parallel surfaces.

pressure on the left and the pressure of p on the right. The oil velocity profile shown with arrow is the result of both the shear flow and the pressure flow. The shear flow is caused by the relative motion between two layers and the pressure flow is due to the pressure difference on two sides [19]–[21].

The velocity of the fluid in the current coordinate u is

$$u = \frac{U}{h}y + \frac{1}{2\mu}\frac{\partial p}{\partial x}(y^2 - yh) \tag{7}$$

where U is the velocity of the upper layer, h is the thickness of the oil film, x and y are the coordinates in the oil film, μ is the oil viscosity, and $\frac{\partial p}{\partial x} = \frac{p}{L}$ is the pressure gradient along the x-axis.

The first term on the right of (7) is the velocity caused by the shear flow, and the second term is the velocity caused by the pressure flow.

According to Newton's law of viscosity, the shear stress on the upper layer τ_h is

$$\tau_h = \mu\frac{du}{dy}|_{y=h} = \mu\frac{U}{h} + \frac{ph}{2L}. \tag{8}$$

The viscous force acting on the upper layer F_v is

$$F_v = \tau_h Lb = \mu\frac{Lb}{h}U + \frac{hb}{2}p. \tag{9}$$

There are two terms on the right of (9). The first term is the viscous force due to the relative motion between two layers. The second term is the viscous force caused by the pressure gradient within the oil film.

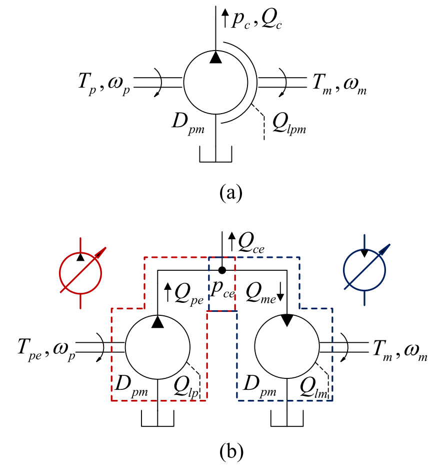

Fig. 4. PCT and its equivalent HST. (a) PCT. (b) Equivalent HST.

For the oil film regions in the inlet or outlet chamber, there are no pressure gradients within the oil films, and the viscous forces are caused only by the relative motion between the two layers. The oil film regions between the inlet and outlet chambers are transition regions. There are pressure gradients in these regions, either from high to low pressure or from low to high pressure [22]. The viscous forces in these regions are caused by both the relative motion between the two layers and the pressure gradients.

The viscous forces caused by the relative motion of the two layers in the oil film are equal and opposite. For the layer with a higher speed, the viscous force slows it down. For the layer with a lower speed, the viscous force speeds it up. Since the rotor speed is always higher than the ring speed, the viscous force acts as a drag force on the rotor and a drive force on the ring. This is the essential reason why the PCT is more efficient than a conventional HST.

Due to the complexity of the ring inner contour and the pressure distribution along the ring inner surface, it is difficult to calculate the viscous torque from the viscous stress distribution along the ring inner surface. To accurately determine the viscous torque on the floating ring, a 3-D CFD model taking mechanical and fluid domains simulation into considerations is required. Similar to the pressure induced torque, this viscous torque between the rotor and the floating ring acts as a load torque on the input shaft and a driving torque on the output shaft.

D. Transmission Efficiency

The PCT and its equivalent HST are shown in Fig. 4. In the PCT, the pumping and motoring functions are achieved in one unit. In its equivalent HST, the pumping and motoring functions are achieved in two separate units—pump and motor. The equivalent HST differs from a conventional HST in that it has a control port to adjust the transmission ratio. As shown in the figure, a fixed displacement pump with a control port achieves the same variable function as a variable displacement pump in a conventional HST. In the same way, a fixed displacement motor with a control port achieves the same variable function as a variable displacement motor in a convention HST. In a conventional variable pump or motor, the variable function is achieved by mechanical design, while in the equivalent variable unit, the variable function is achieved by the pressure control. The fixed displacement pump and motor have the same displacements as the PCT (D_{pm}).

To show the advantage of the PCT, the drive efficiencies of the two transmissions are compared. In the analysis, the two transmissions have the same output torque and speed (T_m, ω_m). The two transmissions are controlled so that they have the same input speed (ω_p) but different input torque. The drive efficiencies are compared though the different input torques.

The control flow in the PCT Q_c is

$$Q_c = (\omega_p - \omega_m)\, D_{pm} - Q_{lpm} \tag{10}$$

where Q_{lpm} is the leakage in the PCT.

In the equivalent HST, the control flow Q_{ce} is

$$Q_{ce} = Q_{pe} - Q_{me} = (\omega_p - \omega_m)\, D_{pm} - (Q_{lp} + Q_{lm}) \tag{11}$$

where Q_{lp} and Q_{lm} are the pump and motor leakage in the equivalent HST.

Since the PCT combines both the pumping and motoring function in one unit, it is reasonable to assume that its leakage is smaller than the sum of the pump and motor leakage ($Q_{lpm} < Q_{lp} + Q_{lm}$). Based on (10) and (11), the control flow in the PCT is larger than its equivalent HST ($Q_c > Q_{ce}$).

In the PCT, the input shaft torque is

$$T_p = p_c D_{pm} + T_v + T_{fp}. \tag{12}$$

There are three terms on the right of (12). The first term is the hydraulic torque caused by the control pressure. The second term T_v is the viscous torque acting on the rotor. The third term T_{fp} is the friction torque in the pumping unit, mainly the bearing friction torque [23].

The hydraulic torque and the viscous torque drive the output shaft. The output shaft torque of the PCT T_m is

$$T_m = p_c D_{pm} + T_v - T_{fm} \tag{13}$$

where T_{fm} is the friction torque in the motoring unit, mainly the bearing friction torque.

Combining (12) and (13)

$$T_p = T_m + (T_{fp} + T_{fm}). \tag{14}$$

It is shown from (14) that the differences between input and output shaft torques are only the bearing friction torques.

In the equivalent HST, the input shaft torque T_{pe} is

$$T_{pe} = p_{ce} D_{pm} + T_{vp} + T_{fpe} \tag{15}$$

where p_{ce} is the control pressure in the equivalent HST, T_{vp} is the viscous torque in the pump, and T_{fpe} is the friction torque in the pump, mainly the bearing friction torque.

The output shaft torque in the equivalent HST T_m is

$$T_m = p_{ce} D_{pm} - T_{vm} - T_{fme} \tag{16}$$

where T_{vm} is the viscous torque in the motor, and T_{fme} is the friction torque in the motor, mainly the bearing friction torque.

Combining (15) and (16)

$$T_{pe} = T_m + (T_{vp} + T_{vm}) + (T_{fpe} + T_{fme}). \tag{17}$$

Since the friction torques in the pump and motor T_{fpe} and T_{fme} are mainly the bearing friction torques, it is reasonable to assume that the bearing friction torques are the same in the two transmissions ($T_{fp} = T_{fpe}$ and $T_{fm} = T_{fme}$).

Comparing (14) and (17)

$$T_p < T_{pe}. \tag{18}$$

In the analysis, the two transmissions have the same output torque and speed. The two transmissions are controlled so that they have the same input speed but different input torque. Equation (18) shows that the input torque of the PCT is lower than its equivalent HST. This indicates that the PCT has higher drive efficiency than its equivalent HST. It is shown from (14) and (17) that the input shaft torque difference between the two transmissions comes from the viscous torque in the pump and motor in the HST ($T_{vp} + T_{vm}$). In the PCT, the viscous torques in the pumping and motoring unit are internal torques. In the equivalent HST, the viscous torque in the pump is not transmitted to the motor [24]. Instead the power from this torque is dissipated as heat. This torque does not do useful work since the pump and motor cases are stationary.

Some studies have been conducted on conventional double-acting vane pumps. A theoretical analysis on the mechanical efficiency of a double-acting vane pump is presented in [25]–[27], with the focus on the friction torque reduction through both the parameter design and the structure optimization. Cho *et al.* [28] investigated the lubrication mode of the line contacts between the vane tips and the cam ring in a balanced vane pump. Karmel [29], [30] presented an analysis of the force and torque applied to the cam ring, shaft, and the vanes in a single-acting variable displacement vane pump. Although these studies are based on conventional vane pumps, the friction and torque analysis between the vane tips and the cam ring gives a good understanding on how the PCT works.

III. Experimental Study

To demonstrate its advantage, the prototype of the new transmission is built and tested in a fan drive system. The PCT is built or modified from a commercial double-acting vane pump with the displacement of 68 cm^3/rev. Except for the rotating Q1 ring assembly, the basic structure of the PCT is the same as the commercial vane pump. The drive efficiency of the PCT is compared with a conventional HST consisting of a variable displacement pump and a fixed displacement motor. To conduct a fair comparison, the pump and motor used in the conventional HST test are also vane types. A 40 cm^3/rev variable displacement vane pump and a 32 cm^3/rev variable displacement motor held at maximum displacement are used in the HST test. The experimental study is conducted in two steps: 1) use a variable frequency drive (VFD) electric motor to drive a fan and measure the VFD power draws at different fan speeds; 2) set the PCT and the conventional HST between the VFD motor and the fan, respectively, and, then, compare the VFD power draws with

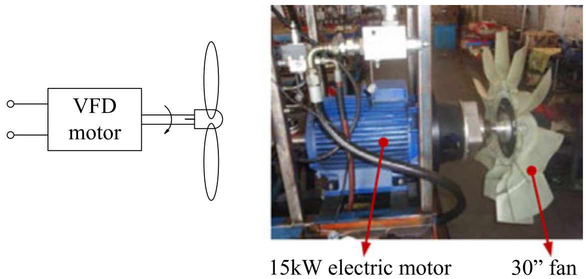

Fig. 5. Direct fan drive using a VFD motor.

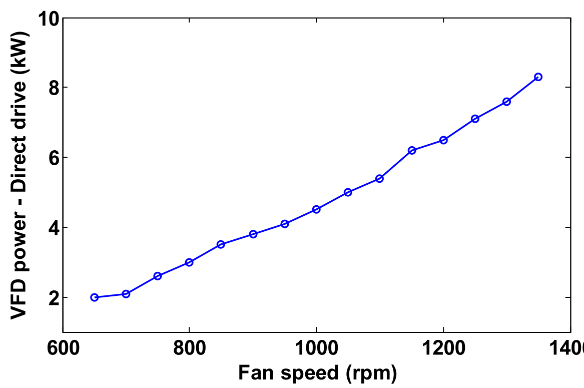

Fig. 6. VFD power draw at the different fan speeds—Direct drive.

the two transmissions. The first step is the baseline test and the second is the comparison test.

A. Baseline Test

The schematic of the baseline test is shown in Fig. 5. It uses a VFD electric motor to drive a 30″ plastic fan directly. This 30″ plastic fan is the cooling fan for the Mack MP8 470 hp diesel engine.

The rated power of the electric motor is 15 kW. The VFD power draw is the electric power to the motor and can be read from the VFD controller. The baseline test is to get the VFD power draw at the different fan speeds. The VFD power draws at the different fan speeds are shown in Fig. 6.

B. Comparison Test

To conduct a fair comparison, the two fan drive systems have the same fan speed (output speed) and VFD speed (input speed). Since the fan shaft torque is proportional to the square of the fan speed according to the fan law, the output torques of the two systems are also the same. The efficiency discrepancy between the two transmissions is therefore reflected by the different input torque or power to the system. This is the same condition set in the transmission efficiency analysis section.

The fan drive comparison tests with two transmissions are shown in Fig. 7. Fig. 7(a) shows the test with an HST consisting of a variable displacement pump and a fixed displacement motor, Fig. 7(b) shows the test with the PCT, where the pressure is controlled by a pressure relief valve.

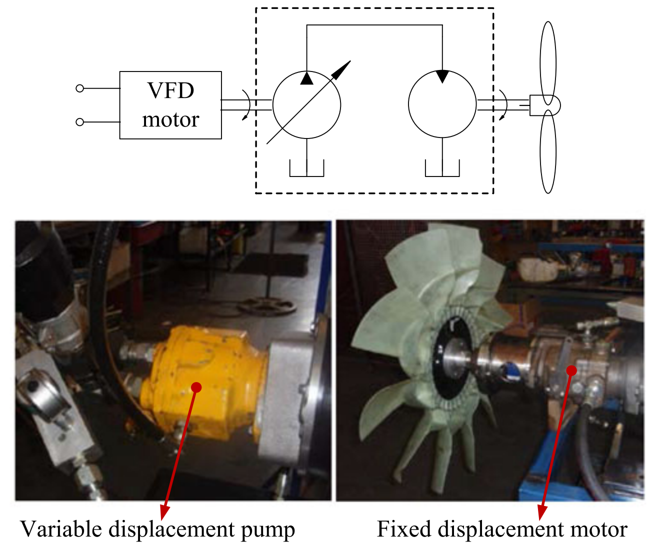

(a)

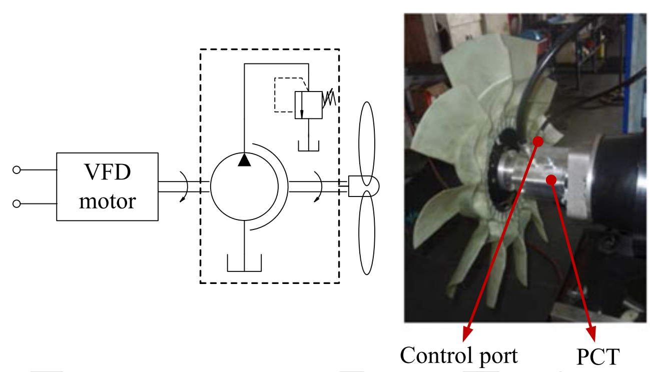

(b)

Fig. 7. Fan drive comparison tests with PCT and conventional HST (same fan speeds and VFD speeds). (a) Fan drive with HST. (b) Fan drive with PCT.

TABLE I
FAN DRIVE COMPARISONS WITH DIFFERENT TRANSMISSIONS

VFD speed (r/min)	Fan speed (r/min)	VFD power draw (kW)				
		HST (baseline)	PCT	HST minus PCT	PHMT	HST minus PHMT
1400	900	4.8	4.4	0.4	4.4	0.4
1400	1000	6.2	5.0	1.2	4.8	1.4
1400	1100	7.4	5.9	1.5	5.8	1.6
1400	1200	8.9	7.2	1.7	7.0	1.9
1400	1300	10.8	8.6	2.2	8.3	2.5

The VFD power draw comparisons with two transmissions are shown in Table I. The input speeds (VFD speed) of the two systems are set constant at 1400 r/min. In the system with HST, the fan speed is adjusted by controlling the pump displacement. The fan speed is adjusted by controlling the pressure in the system with PCT. Results show that the VFD power draw with PCT is lower than that with HST at different fan speeds, which is consistent with the analysis results.

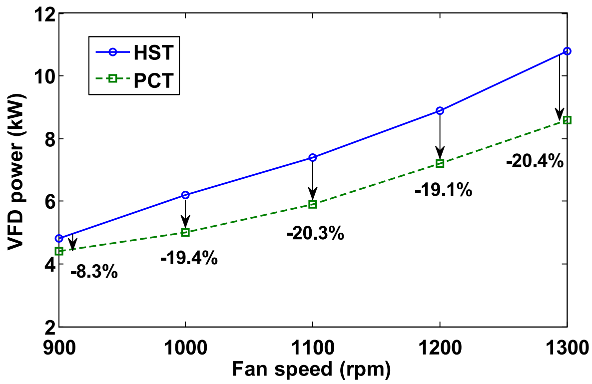

Fig. 8. VFD power draws with PCT and HST at different fan speeds.

It is also shown in Table I that the VFD power draw saving (in kilowatt) with PCT (from HST baseline) increases with the fan speed. As the fan speed increases, the differential speed between input and output shaft in the PCT decreases, since the VFD speed is constant. This results in a reduced control flow in the PCT. Although the fan shaft torque or control pressure increases with the fan speed, the reduced control flow enlarges the energy saving benefit in the PCT as the fan speed increases. The VFD power draws with PCT and HST at different fan speeds are shown in Fig. 8.

It is important to determine the PCT displacement correctly in the fan drive system. The fan power is proportional to the cube of the fan speed and the fan shaft torque is proportional to the square of the fan speed. The maximum fan shaft torque is at the maximum fan speed. The PCT displacement is determined by the maximum fan shaft torque and the PCT operating pressure.

To make the PCT more efficient in the fan drive system, the hydraulic power at the control port is harvested and fed into a hydraulic motor coupled to the output shaft of the PCT. This turns the PCT to a pressure-controlled hydromechanical transmission (PHMT). The fan drive test with the PHMT is shown in Fig. 9.

The fan drive test with the PHMT is set the same as the HST and PCT tests, where the VFD speed keeps constant. In the PHMT test, the same 68 cm^3/rev PCT and the same motor used in the HST test but with variable displacement are used. The VFD power draw with the PHMT is compared with the results with the HST and the PCT in Table I. It is shown that the VFD power draw with the PHMT is lower than that with PCT but the difference is small. The VFD power draws with the PHMT and the PCT at different fan speeds are compared in Fig. 10. The small VFD power draw difference in the figure may come from either low PCT output flow, motor inefficiency, or a combination of the two.

IV. Conclusion

An efficient fan drive system based on a novel PCT is introduced in this paper. The new transmission combines pumping and motoring functions in one unit, making it simpler than a conventional HST. Unlike a conventional HST, the transmission ratio of a PCT is adjusted by controlling the pressure. The control

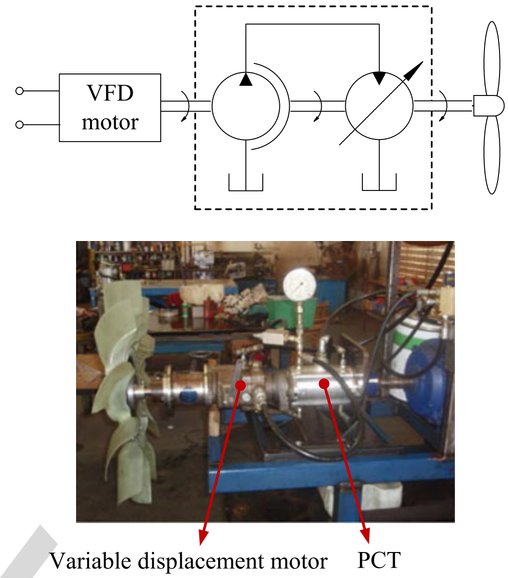

Fig. 9. Fan drive test with PHMT.

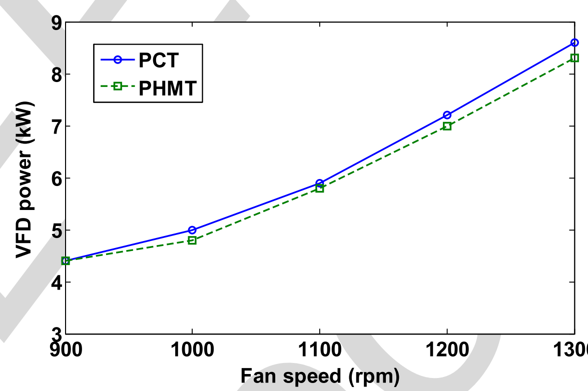

Fig. 10. VFD power draws with PHMT and PCT at different fan speeds.

flow is determined by the differential speed between the input and output shaft.

There are two driving torques acting on the output shaft of the PCT, the hydraulic torque and the viscous torque. The hydraulic torque is the pressure induced torque, which is the product of the control pressure and the PCT displacement. In a conventional vane pump or motor, the viscous torque power turns into heat since the ring is stationary. In the PCT, the viscous torque is transmitted through the floating ring to the output shaft, thus increasing the efficiency. This is the essential reason why the PCT is more efficient than a conventional HST.

The PCT is applied to a fan drive system, and the transmission efficiency is compared to a conventional HST consisting of a variable displacement pump and a fixed displacement motor. Experimental results show that the input power with the PCT is lower than that with an HST given the same input speed and fan speed.

To make the PCT more efficient in the fan drive system, the hydraulic power at the control port can be harvested and fed into a hydraulic motor coupled to the output shaft of the PCT.

This turns the PCT into a PHMT and experimental result shows higher transmission efficiency than a PCT.

Acknowledgment

The authors would like to acknowledge the technical support in the testing from N. Mathers and R. Price of Mathers Hydraulics, and the helpful discussions with M. Gust of CCEFP.

References

[1] "Final regulatory analysis: Control of emissions from nonroad diesel engines", U.S. Department of Energy, Washington, DC, USA, Tech. Rep. EPA420-R-04-007, May 2004.

[2] S. Niemi, K. Lundin, T. Karhu, M. Laure´n, K. Ekman, P. Nousiainen, and T. Paanu, "Exhaust particle number in off-road engines of different generations," SAE, Warrendale, PN, USA, Tech. Paper 2009-01-1869sae, 2009.

[3] P. Setlur, J. Wagner, D. Dawson, and E. Marotta, "An advanced engine thermal management system: Nonlinear control and test," *IEEE/ASME Trans. Mechatronics*, vol. 10, no. 2, pp. 210–220, Apr. 2005.

[4] M. H. Salah, T. H. Mitchell, J. R. Wagner, and D. M. Dawson, "A smart multiple-loop automotive cooling system—Model, control, and experimental study," *IEEE/ASME Trans. Mechatronics*, vol. 15, no. 1, pp. 117–124, Feb. 2010.

[5] *Improving Fan System Performance: A Sourcebook for Industry*. Washington, DC, USA: U.S. Department of Energy, Apr. 2003.

[6] J. Eberth, J. Wagner, B. Afshar, and R. Foster, "Modeling and validation of automotive "smart" thermal management system architecture," SAE, Warrendale, PN, USA, Tech. Paper 2004-01-0048, 2004.

[7] R. Henry, J. Koo, and C. Richter, "Model development, simulation and validation, of power train cooling system for a truck application," SAE, Warrendale, PN, USA, Tech. Paper 2001-01-1731, May 2001.

[8] H. Cho, D. Jung, Z. Filipi, and D. Assanis, "Application of controllable electric coolant pump for fuel economy and cooling performance improvement," in *Proc. ASME Int. Mech. Eng. Congr. Expo.*, Anaheim, CA, USA, Nov. 2004, vol. 44, pp. 43–50.

[9] F. P. Bleier, *Fan Handbook: Selection, Application, and Design*. New York, NY, USA: McGraw-Hill, 1998.

[10] R. Chalgren, Jr., and D. Allen, "Light duty diesel advanced thermal management," SAE, Warrendale, PN, USA, Tech. Paper 2005-01-2020, May 2005.

[11] R. Chalgren, Jr., and T. Traczyk, "Advanced secondary cooling systems for light trucks," SAE, Warrendale, PN, USA, Tech. Paper 2005-01-1380, Apr. 2005.

[12] A. Choukroun and M. Chanfreau, "Automatic control of electric actuators for an optimized engine cooling thermal management," SAE, Warrendale, PN, USA, Tech. Paper 2001-01-1758, May 2001.

[13] M. Salah, P. Frick, J. Wagner, and D. Dawson, "Hydraulic actuated automotive cooling systems—Nonlinear control and test," *Control Eng. Pract.*, vol. 17, no. 5, pp. 609–621, 2009.

[14] A. Al-Jarrah, M. Salah, and A. Al-Tamimi, "Variable structure control schemes for hydraulic actuated automotive cooling systems," in *Proc. 9th Int. Symp. Mechatron. Appl.*, Amman, Jordan, Apr. 9–11, 2013.

[15] H. Merritt, *Hydraulic Control Systems*. New York, NY, USA: Wiley, 1967.

[16] J. Korn, *Hydrostatic Transmission Systems*. London, U.K.: Intertext Books, 1969.

[17] N. Mathers, "Hydrostatic torque converter and torque amplifier," U.S. Patent 20 130 067 899 A1, Mar. 21, 2013.

[18] R. P. Lambeck, *Hydraulic Pumps and Motors—Selection and Application for Hydraulic Power Control Systems*. New York, NY, USA: Dekker, 1983.

[19] A. Cameron, *Basic Lubrication Theory*, 3rd ed. New York, NY, USA: Halsted Press 1981.

[20] R. C. Binder, *Fluid Mechanics*, 3rd ed. New York, NY, USA: Prentice-Hall, 1955.

[21] W.A. Gross, *Fluid Film Lubrication*. New York, NY, USA: Wiley, 1980.

[22] J. Watton and K. L. Watkins-Franklin, "The transient pressure characteristic of a positive displacement vane pump," *Proc. Inst. Mech. Part A, J. Power Energy*, vol. 204, no. 4, pp. 269–275, 1990.

[23] W. E. Wilson, "Rotary-pump theory," *Trans. ASME*, vol. 68, no. 4, pp. 371–384, 1946.

[24] A. Hibi and T. Ichikawa, "Mathematical model of the torque characteristics for hydraulic motors," *Bull. JSME*, vol. 20, no. 143, pp. 616–621, 1977.

[25] Y. Inaguma, "Theoretical analysis of mechanical efficiency in vane pump," JTEKT Eng. J. English Tech. Paper 1007E, pp. 28–35, 2010.

[26] Y. Inaguma and A. Hibi, "Vane pump theory for mechanical efficiency," *Proc. Inst. Mech. Eng. Part C, J. Mech. Eng. Sci.*, vol. 219, pp. 1269–1278, 2005.

[27] Y. Inaguma and A. Hibi, "Reduction of friction torque in vane pump by smoothing cam ring surface," *Proc. Inst. Mech. Eng. Part C, J. Mech. Eng. Sci.*, vol. 221, pp. 527–534, 2007.

[28] I. S. Cho, S. H. Oh, K. K. Song, and J. Y. Jung, "The lubrication characteristics of the vane tip under pressure boundary condition of oil hydraulic vane pump," *J. Mech. Sci. Technol.*, vol. 20, no. 10, pp. 1716–1721, 2006.

[29] A. M. Karmel, "A study of the internal forces in a variable-displacement vane-pump—Part I: A theoretical analysis," *ASME J. Fluids Eng.*, vol. 108, no. 2, pp. 227–232, 1986.

[30] A. M. Karmel, "A study of the internal forces in a variable-displacement vane-pump—Part II: A parametric study," *ASME J. Fluids Eng.*, vol. 108, no. 2, pp. 233–237, 1986.

Feng Wang received the B.S., M.S., and Ph.D. degrees in mechanical engineering from Zhejiang University, Hangzhou, China, in 2003, 2005, and 2009, respectively.

In 2003, he became a Research Assistant at the Department of Mechanical Engineering and the State Key Laboratory of Fluid Power Transmission and Control, Zhejiang University. In 2009, he became a Postdoctoral Associate at the Department of Mechanical Engineering, University of Minnesota, Minneapolis, MN, USA, where he joined the NSF Engineering Research Center for Compact and Efficient Fluid Power. His current research interests include modeling and control of hydrostatic drives, hydrostatic wind turbines, hydraulic hybrid vehicles, and applications of hydraulic systems in renewable energy.

Kim A. Stelson received the B.S. degree in mechanical engineering from Stanford University, Stanford, CA, USA, in 1974, and the S.M. and Sc.D. degrees in mechanical engineering from the Massachusetts Institute of Technology, Cambridge, MA, USA, in 1977 and 1982, respectively.

He is currently the Director of the NSF-funded Engineering Research Center for Compact and Efficient Fluid Power, University of Minnesota, Minneapolis, MN, USA, where has been a Professor at the Department of Mechanical Engineering since 1981. His fluid power research interest includes work on hydraulic hybrid vehicles and hydrostatic transmissions for wind power. Before working in fluid power research, he was active in research in the modeling and control of manufacturing processes, especially metal forming, polymer processing, and composite materials manufacturing. He has been a Visiting Faculty Member at the Hong Kong University of Science and Technology, the University of Auckland, and the University of Bath. He has previously been the Director of the Design and Manufacturing Division and the Director of Graduate Studies for the M.S. in Manufacturing Systems Program at the University of Minnesota.

Prof. Stelson has been an Associate Technical Editor of the *Journal of Dynamic Systems, Measurement and Control*, a journal that has twice received the Rudolf Kalman Best Paper Award. He is a Fellow of the American Association for the Advancement of Science.

QUERIES

Q1. Author: “cc/rev” has been changed to “cm^3/rev” here and elsewhere in the text. Please check.

Q2. Author: Please verify Refs. [1] and [19] as set.